Asian Engineering Review
ISSN: 2409-6725
Vol. 2, No. 1, 1-14, 2015
http://asianonlinejournals.com/index.php/AER

Effects of a Non-Sinusoidal Wind on Plants

Y. L. Makenne[1] --- R. Kengne[2] --- F. B. Pelap[3]*

[1,2,3]Laboratoire de Mécanique et de Modélisation des Systèmes Physiques (L2MSP), Faculté des Sciences, Université de Dschang, Cameroun.

Abstract

In this paper, we elaborate a nonlinear theory of plants suggested to both fifth nonlinearities and non-sinusoidal wind effects modeled by the sinus cardinal function known as a good model used to approximate the Dirac function (behavior). By using the plan beam theory and the multiple time scales method, we find that the interactions between plants and wind are governed by the coupled differential system of equations. Through analytical and numerical techniques, we observe in the non-resonance state, that the effects of wind on the plant are worthless while its harmonic oscillations with their corresponding stability boundaries are tackled in the resonance case. Owing to the rang of the control parameters, we also examine periodic, quasi-periodic and chaotic behavior of the system. Our investigations show that judicious choice of some system's parameters can avoid the plant rupture during violent storms. For applications, numerical simulations carry out with the physical parameters of Pinus Pinaster Ait., corn plant and those of Raphia Vinifera lead to very interesting results showing the wideness applicability of the results established within this paper.

Keywords: Plants, Nonlinear dynamics, Resonance, Stability, Chaotic behavior, Non-sinusoidal wind load, Hysteresis, Applications.

This work is licensed under a Creative Commons Attribution 3.0 License
Asian Online Journal Publishing Group

Contents

* *Corresponding Author*

1. Introduction

Several studies have been reported in the investigation of the wind-plant interactions [1-4] since wind damage is a global phenomenon that affects plantations and forests such as Storm Vivian in Northern Europe [5]. Such storms severely affect forest management in many countries of the world [6]. Wind loads are understood as a largest dynamic load on plants [7-9]. Loads caused by wind are periodic and create a sway motion in trees which can be simplified using a conceptual model of a tree stem without branches and being considered as an upside-down pendulum or a beam [10, 11]. In this context various studies regard the wind-plant interaction as linear [12] by considering the plant's stem as an elastic rod excited by wind. Wherein, Tchassi has found that the plant amplitude of oscillations increases not only with the density of field but also with the average speed of the wind showing that this speed varies rapidly with time. On the other hand, those studies consider the wind profile as sinusoidal [12, 13]. In particular, this last research work has the feature of introducing the nonlinear behavior of the wind-plant interaction but takes a sinusoidal wind profile. This sinusoidal form is known to be a school case which is very difficult to realize since a signal produced by the real physical system cannot exist at infinite**.** Likewise a pure sinusoidal physical phenomenon does not exist since any physical phenomenon has a finite duration.

In this paper, we proposed to improve this last work by considering nonlinear wind-plant interactions suggested to sinus cardinal wind profile since it is known that external excitation possesses a sinus cardinal profile is currently used in mathematical/numerical analysis, wave physics and numerical digital signal [14-17]. This paper is organized as follows**.** Section 2 presents the model description as well as the nonlinear damped coupled equations of motion. Section 3 investigates the analytical and numerical solutions of the concerned system. Section 4 deals with the study of the chaotic behavior of our system while discussion and concluding remarks are given in section 5.

2. Model Description and Equations of Motion

During the plant existence, its dynamical characteristics are decisive elements for his interaction with the environment (wind for example). The movement of air in the absence of obstacles is described by the general fluid equation [18]. In our study of the interactions between air and plants, we assume that the velocity field is homogeneous with uniform motion in the x-direction and the force per volume unit is neglected. Therefore, the equation of the air motion is reduced to the following differential equation that links the wind acceleration to the pressure gradient :

$$\frac{dv}{dt} = -\frac{1}{\rho}\frac{dp}{dx} \tag{1}$$

where p is the pressure, ρ the density and t the time of air flow.

To study the dynamics of the plant in the air, we exploit the classical dynamics theory of beams [5] and obtain the following system of coupled nonlinear differential and damped dimensionless equations that governs the plant's motion in the air :

$$\frac{d^2x}{d\tau^2} + \mu_1\frac{dx}{d\tau} + \omega_0^2 x + \gamma x^3 + \lambda x^5 = \alpha_1\left(v - \frac{dx}{dt}\right)\left|v - \frac{dx}{dt}\right| \tag{2a}$$

$$\frac{dv}{dt} + \beta_1\left(v - \frac{dx}{dt}\right)\left|v - \frac{dx}{dt}\right| = K(\tau) \tag{2b}$$

wherein x is the amplitude of the plant displacement, v is the fluctuated values of the wind speed, α_1 and β_1 are constants coefficients, ω_0 is the natural frequency of the plant, γ and λ are respectively the cubic and fifth order nonlinear coefficients, and μ_1 is a damping coefficient. In Eqs.(2), $K(\tau)$ stands for the wind action on the plant and its explicit form will influence the motion adopted by the plant. Hence, $K(\tau)$ could have a sinusoidal form, a sinus cardinal behavior or a stochastic form. However, the sinusoidal signal [13] is a school case which is very difficult to realize since the signal produced by the real physical system cannot exist at infinite. Likewise a pure sinusoidal physical phenomenon does not exist since any physical phenomenon has a finite duration. In the present investigations, we consider that the external excitation possesses a sinus cardinal profile ($K(\tau) = K_1 \sin c(\omega\tau)$) which is currently used in numerical digital signal [14], wave physics [15] and mathematical/numerical analyses[16, 17]. This sinus cardinal profile is also very useful because it is possible to exploit the Dirac function to represent its impulsion for small time [19, 20]. This form of the external excitation is requested when the amplitude of the wind is concentrated on the specific part of the plant. Here, K_1 is the amplitude of the external excitation strength. Consequently, Eqs. (2) are rewritten as :

$$\frac{d^2x}{d\tau^2} + \mu_1\frac{dx}{d\tau} + \omega_0^2 x + \gamma x^3 + \lambda x^5 = \alpha_1\left(v - \frac{dx}{dt}\right)\left|v - \frac{dx}{dt}\right| \tag{3a}$$

$$\frac{dv}{dt} + \beta_1\left(v - \frac{dx}{dt}\right)\left|v - \frac{dx}{dt}\right| = K_1 \sin c(\omega\tau) \tag{3b}$$

The first equation of (3) describes the plant oscillations under the wind effects and its right hand side defines the drag term while the second equation of the system governs the movement of the wind in the presence of the plant associated with the drag per unit mass. Let us remind that the sources of friction of a vibrating plant in the air possess three main origins: the interactions between the given plant and the neighboring plants, changes in aerodynamic movement of foliage, the natural viscosity of the plant under consideration. Since we consider the drag term, which is in general the trajectory described in the air or on the surface by the body in motion, we will study the changes in the aerodynamic movement of foliage. In relations (3), $\alpha_1 = C_p s/(2S\omega_0)$ and $\beta_1 = C_a A/2$ are constant coefficients

in which C_a is a positive constant that characterizes the trajectory of the plant during its motion in the air (drag), $A = S/\Omega$ designates a spatial area per unit volume projected normally to the wind direction, Ω stands for the volume of air, s is the cross section of the plant, S represents the projected area on the perpendicular plane of air flow of the deformed stalk that could depend on the plant's height or its length, C_p is the drag coefficient of the deformed plant linked to its geometry. Therefore, we may expand the nonlinear product within (3) to the third order as follows

$$\left(v-\frac{dx}{dt}\right)\left|v-\frac{dx}{dt}\right| \approx c_1\left(v-\frac{dx}{dt}\right)+c_2\left(v-\frac{dx}{dt}\right)^3$$

in which c_1 and c_2 are real constants and $v-\dfrac{dx}{dt}$ is the relative speed of air in relation to plant. Consequently, expressions (3) take the form:

$$\frac{d^2x}{d\tau^2}+\left(\mu_1+\alpha_1 c_1\right)\frac{dx}{d\tau}+\omega_0^2 x+\gamma x^3+\lambda x^5-\alpha_1 c_1 v-\alpha_1 c_2\varepsilon^2\left(v-\frac{dx}{dt}\right)^3=0 \qquad (4a)$$

$$\frac{dv}{dt}+\beta_1 c_1 v-\beta_1 c_1\frac{dx}{dt}+\beta_1 c_2\varepsilon^2\left(v-\frac{dx}{dt}\right)^3=K_1\sin c\left(\omega\tau\right) \qquad (4b)$$

These relations represent the coupled system of nonlinear differential damped equations that governs the plant-wind interactions.

3. Analysis of the Equations of Motion

The aim of this section is to investigate the analytical and numerical solutions of the equations of motion (4). Thus, there exist several methods to solve analytically these equations. Since we are interested by weak displacements of the plant, we choose the multiple time scales (MTS) method [18] for this analysis. For this purpose, we multiply the amplitude of the external force by ε and the damping coefficients by ε^2 in order to ensure the nonlinear factor to appear simultaneously with friction and the external excitation. This last assumption also allows the determination of certain greatness characteristics of the system plant-wind. Hence, we put $\alpha_1=\varepsilon^2\alpha$, $\beta_1=\varepsilon^2\beta$, $\mu_1=\varepsilon^2\mu$ and $K_1=\varepsilon K_0$. Under all these considerations, the equations describing the motion of the system take the form:

$$\frac{d^2x}{d\tau^2}+\varepsilon^2\left(\mu+\alpha c_1\right)\frac{dx}{d\tau}+\omega_0^2 x+\gamma x^3+\lambda x^5-\varepsilon^2\alpha c_1 v-\alpha c_2\varepsilon^2\left(v-\frac{dx}{d\tau}\right)^3=0 \qquad (5a)$$

$$\frac{dv}{d\tau}+\beta c_1 v-\varepsilon^2\beta c_1\frac{dx}{d\tau}+\beta c_2\varepsilon^2\left(v-\frac{dx}{d\tau}\right)^3=\varepsilon K_0\sin c\left(\omega\tau\right) \qquad (5b)$$

Following the MTS method, the general solution of Eqs. (5) is expanded as:

$$x(t,\varepsilon)=x_0\left(T_0,T_1\right)+\varepsilon x_1\left(T_0,T_1\right)+\varepsilon^2 x_2\left(T_0,T_1\right)+\ldots \qquad (6a)$$

$$v(t,\varepsilon)=v_0\left(T_0,T_1\right)+\varepsilon v_1\left(T_0,T_1\right)+\varepsilon^2 v_2\left(T_0,T_1\right)+\ldots \qquad (6b)$$

in which ε is a small dimensionless perturbative parameter that helps to control the order of the amplitude of oscillations. The fast time scale T_0 and the slow time scale T_1 characterize the modulations in the amplitude and phase of the solutions (x,v) induced by nonlinearities, damping and coupling of the considering system. Substituting the expressions (6) into Eqs.(5) and equating the coefficients of ε^0 and ε^1 to zero, lead to the following systems of equations for x_j and v_j $(j=0,1)$:

Order ε^0 :

$$D_0{}^2x_1+\omega_0{}^2x_1=0 \qquad (7a)$$

$$D_0v_1+\beta c_1v_1=K_0\sin c(\omega T_0) \qquad (7b)$$

Order ε^1 :

$$D_0{}^2x_3+\omega_0{}^2x_3=-2D_0D_2x_1-2\mu_2D_0x_1-\gamma x_1+\alpha c_1v_1+\alpha c_2v_1{}^3 -3\alpha c_2v_1{}^2(D_0x_1)+3\alpha c_2v_1(D_0x_1)^2-\alpha c_2(D_0x_1)^3 \qquad (8a)$$

$$D_0v_3+\beta c_1v_3=-D_2v_1+\beta c_1D_0x_1-\beta c_2v_1{}^3+3\beta c_2v_1D_0x_1 -3\beta c_2v_1(D_0x_1)^2+\alpha c_2(D_0x_1)^3 \qquad (8b)$$

with $\mu_2=\left(\mu+\alpha c_1\right)/2$; $D_0=\partial/\partial\tau_0$ and $D_1=\partial/\partial\tau_1$.

The resolution of Eqs. (7) leads to the following general solution

$$x_1=A_1(T_1)exp\{i\omega_0T_0\}\ +\ c.c$$

$$v_1\left(T_0\right)=\alpha_0\,sin\left(\omega T_0\right)-\beta_0\,cos\left(\omega T_0\right)$$

in which $C.C$ stands for the complex conjugate of the preceding terms and diverse constants are given by $\alpha_0 = \alpha(A+B)/T$ and $\beta_0 = \alpha(D+E)/(T_0 c_1)$

with $A = \frac{1}{\omega}\left(\beta + \frac{1}{c_1 T_0}\right)$; $B = \frac{1}{c_1^2}\left(\frac{1}{\beta} + \frac{1}{c_1 T_0}\right)$; $D = \left(\frac{1}{\omega} + \frac{\omega}{\beta^2 c_1}\right)$; $E = \frac{2\omega}{c_1^2 T_0}\left(\beta - \frac{1}{c_1 T_0}\right)$.

Within the solution of Eq. (7a), $A_1(\tau_1)$ represents an arbitrary complex function which is determined from Eq. (7b) by imposing the solvability or secular conditions. Thus, the report of the general solutions x_1 and v_1 into Eq. (8a) yields

$$\begin{aligned} D_0^{\,2} x_3 + \omega_0^{\,2} x_3 = {} & M_1 e^{i\omega_0 T_0} + (M_2 + M_3) e^{i\omega T_0} + (M_4 + M_5) e^{3i\omega T_0} \\ & + M_6 e^{3i\omega_0 T_0} + M_7 e^{i(2\omega+\omega_0)T_0} + M_8 e^{i(\omega+2\omega_0)T_0} \\ & + M_9 e^{i(\omega-2\omega_0)T_0} + M_{10} e^{i(2\omega-\omega_0)T_0} + C.C. \end{aligned} \tag{9}$$

in which the different coefficients M_j $(j = 1,...,10)$ are given in Appendix A. It appears that the right side of Eq. (9) includes both the natural frequency of the plant ω_0 and the frequency of the external excitation (ω). Therefore, it could arise during the plant-wind interactions that these two frequencies are closed (resonance case) or not (non resonance case). These two possibilities will be examined separately in the upcoming subsections.

3.1. Investigation of the Non-Resonant Case

This case appears when the frequency of the external force (wind) is different from the natural frequency of the plant i.e., $\omega \neq \omega_0$. Hence, the solvability conditions applied to Eq. (9) yields

$$-2i\omega_0\left(dA_1/dT_1 + \mu_1 A_1\right) - 3\gamma A_1^2 \overline{A_1} - 3\alpha c_2 \omega_0 A_1\left(\frac{1}{2} i\alpha_2 + \omega_0^{\,2} A_1 \overline{A_1}\right) = 0 \tag{10}$$

in which $\overline{A_1}$ is the complex conjugate of A_1. Assuming weak nonlinearity and using the first order perturbation theory in polar coordinates [21, 22], the solution of Eq. (10) could be taken in the form :

$$A_1(T_1) = \frac{1}{2} a\ (T_1)\ exp\left[i\theta(T_1)\right] \tag{11}$$

where a and θ are real quantities that represent respectively the amplitude and the phase of the oscillations. Substitution of expression (11) into Eq. (10) leads to an equation whose separation in real and imaginary parts in stationary state yields a coupled flow for the amplitude and phase. Resolution of the obtained equations provides the following expressions for a and θ respectively :

$$a = \phi \cdot \sqrt{\frac{\exp(-2NT_1)}{1 - \phi\delta\exp(-2NT_1)}} \quad \text{and} \quad \theta = \frac{3\gamma}{16 N \omega_0 \delta}\ln\left[1 - \phi\delta\exp(-2NT_1)\right] + C_4 \tag{12}$$

with $N = \mu_1 + \frac{3}{4} c_2 \alpha\alpha_2$; $N_1 = \frac{3}{8}\alpha\omega_0^3 c_2$ and $\delta = N/N_1$. The quantities ϕ and C_4 stand for integration constants. Therefore, it becomes possible to write the explicit form of the solution of Eqs. (7) and to check numerically its behavior as exhibited on Fig. 1a. This graph shows that when the time increases, oscillations of the plant stabilize at zero. This result is of weak interest because it describes the state of plant oscillations that disappears with time showing that the wind has no effect on the movement of the plant. To compare this result to that established for the sinusoidal wind profile [12, 13], we plot the corresponding displacement of the plant as function of time (Fig.1b). We note from these curves that the plant oscillation amplitude is lower and vanished quickly in the non-sinusoidal case that in the sinusoidal wind load profile. Let us examine how does the system behaves in the resonant case.

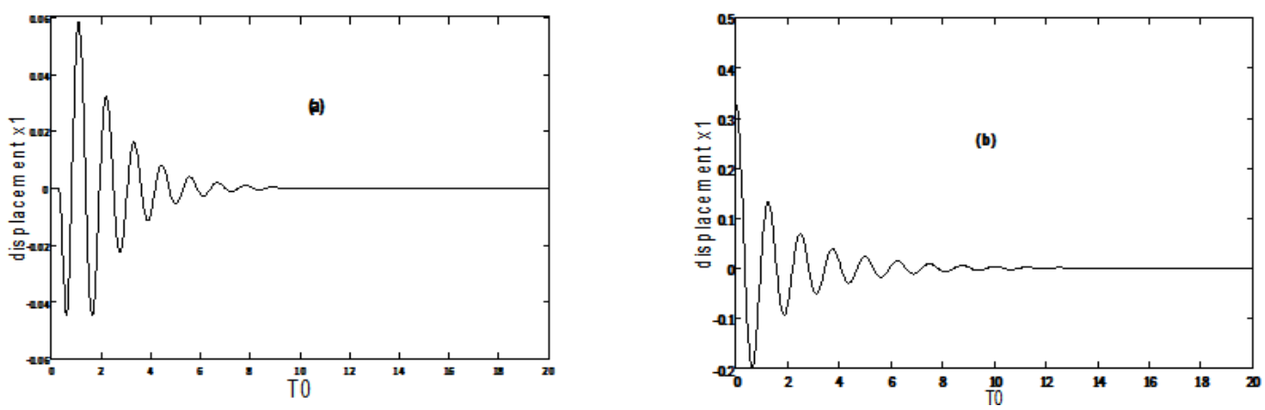

Figures-1. Plant displacements load for the parameters $\alpha = 0.5$, $\mu = 1.1$, $\beta = 17.3$, $\gamma = 15$, $\omega_0 = 5.6$, $c = 0.1$, $\eta = 0.5$ with $T_1 = \varepsilon T_0$. (a): Case of the non-sinusoidal wind load ($K(T_1) = k_0\, sinc(\omega T_1)$) using the parameters $c_1 = 0.7$, $c_2 = 1.5$, $K_0 = 6.3$, $\omega = 35.6$, $\varepsilon = 0.65$ (b): Case of the sinusoidal wind load ($K(T_1) = k_0\, sin(\omega T_1)$) with the parameters $c_1 = 0.01$, $c_2 = 0.05$, $k_0 = 2$, $\omega = 0.5$ and $\varepsilon = 0.55$.

3.2. The Resonant Case

Generally the resonance phenomenon occurs when the external frequency is too closed to the internal frequency. Therefore the system receives energy and oscillates with big amplitude. The plant experiences this resonance phenomenon owing to the energy it receives from the wind during the plant-wind interactions. In mechanics, this phenomenon is hurtful since it is responsible of the system's destruction. For example, it is the case of the branch break or the uprooting of the plant if its proper frequency is closed to that of the wind which provokes the plant oscillation. Hereafter we will investigate respectively the primary resonance (harmonic oscillation : $\omega \approx \omega_0$) and the different cases of the secondary oscillations (super-harmonic and sub-harmonic oscillations).

3.2.1. Harmonic oscillations

In this case, the closeness between the wind frequency ω and the plant oscillation frequency ω_0 is given by the relation $\omega = \omega_0 + \varepsilon^2\sigma$ in which σ is the resonance frequency parameter (detuning parameter). Secular conditions imposed to the right hand side of the Eq. (9) lead to :

$$-2i\omega_0\left(\frac{d^2A_1}{dT_1^2}+\mu_1 A_1\right)-3\gamma A_1\overline{A_1}-3\alpha i\omega_0 A_1\left(\frac{\alpha_2}{2}+c_2{\omega_0}^2 A_1\overline{A_1}\right)+P_1-P_2+\left(P_4-P_3\right)e^{i\sigma T_1}=0 \qquad (13)$$

with $P_1=-\frac{1}{8}\alpha\alpha_2 c_2\left(\beta_0+i\alpha_0\right)$; $P_2=\frac{1}{8}\alpha c_2\left[\beta_2\alpha_0+i\left(\beta_2\beta_0-\gamma_2\alpha_0\right)\right]$;

$P_3=3\alpha c_2\left[\frac{3}{8}\gamma_2\beta_0+{\omega_0}^2 A_1\overline{A_1}\left(\beta_0-i\alpha_0\right)\right]$ and $P_4=\frac{3}{4}i\alpha c_2\omega_0\left(\alpha_2+\beta_2+\gamma_2\right)\overline{A_1}$.

Considering the steady-state conditions $da/dT_1=0$, $d\psi/dT_1=0$ (which corresponds to the singular point of Eq. (13)) and assuming that amplitude and phase vary slowly, one obtains the following coupled relations :

$$d_9 a\cos(2\psi)=\chi_1+\left(g_1-d_8a^2\right)\cos(\psi)-\left(g_2+d_7a^2\right)\sin(\psi) \qquad (14a)$$

$$d_9 a\sin(2\psi)=-\chi_2+\frac{1}{a}\left(g_1+d_8a^2\right)\sin(\psi)-\left(g_2+d_7a^2\right)\cos(\psi) \qquad (14b)$$

in which the diverse coefficients d_j are given in Appendix B.

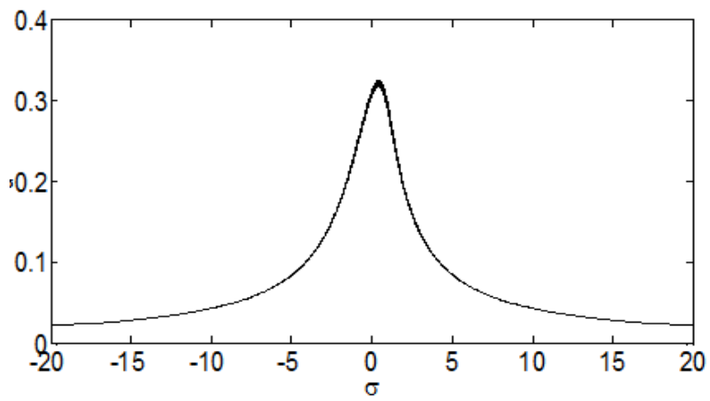

Figure-2. Resonance of the primary state for the parameters $c_1=0.6$; $c_2=0.02$; $\mu=0.05$; $\alpha=4.5$; $\beta=0.1$; $\omega_0=2$; $K_0=1.5$ and $\gamma=25$

The computation of (14) leads to the upcoming algebraic nonlinear equation for the amplitude :

$$A_0a^6+A_{11}a^5+A_2a^4+A_3a^3+A_4a^2+A_5a+A_6=0 \qquad (15)$$

where the different coefficients A_{ij} are given in Appendix C. This expression (called the frequency-response equation) is an implicit function of the detuning parameter σ and the amplitude of the wind load K_0. It cannot be solved analytically. Numerical solution of Eq. (15) presented on Fig.2 gives the behavior of the amplitude at the steady-state. It shows that this amplitude reaches its maximum value when the detuning parameter becomes null. Around this particular value could be observed the destruction of the plant (branch breaking, uprooting, etc.).

To reduce the phenomenon described above, we investigate the impact of the nonlinear terms on the behavior of the block. Owing on the fact that nonlinearity induces generation of harmonics in the system, we wish that, in the presence of higher nonlinearities, the plant could be able to adjust its orientation according to the wind direction. Figs. 3 exhibit the evolution of the amplitude of the plant as function of the detuning parameter σ for various values of the highest nonlinear coefficient γ. We observe hysteresis phenomenon which traduces the capacity of the plant to come back toward the wind profile in a given region and adjust itself to resist the wind attacks. This hysteresis phenomenon clearly comes out for higher nonlinearities.

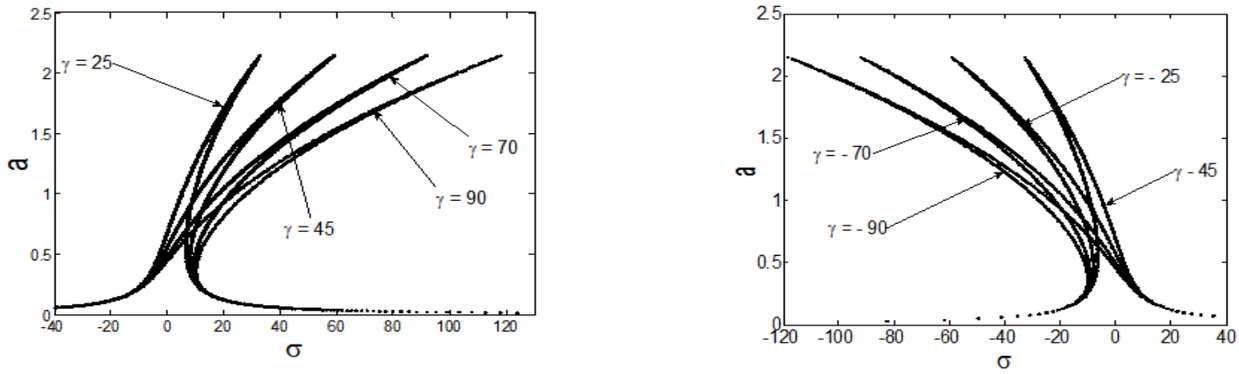

Figure-3. Hysteresis curves obtained at the resonance for the parameters of Fig. 2 with $c_1 = 0.6$, $c_2 = 0.02$, $\beta = 0.18$, $\omega_0 = 2.0032$, $\alpha = 4.5$, $K_0 = 1.902$, $\mu = 0.05$ and several values of γ. The hysteresis phenomenon becomes more visible with the growth of γ values.

Hereafter, we investigate the influence of the other parameters of the system on the amplitude of plant's displacement. Graphs of Figs. 4 give the amplitude-response curves of the harmonic resonance as function of those parameters.

In Fig. 4(a), the effects of the wind amplitude K_0 on the dynamics of the plant are checked. It appears that the acuteness of the resonance increases with the growth of the wind load. Meanwhile, the growth of K_0 is bad for the plant survival. Fig. 4(b) shows that the amplitude of the plant displacement decreases strongly with the increment of the natural frequency of the plant. Since this parameter deals with the mechanical properties of the plants, this result confirms the fact that flexible plants resist well to the wind attacks. On Fig. 4(c), the influence of the parameter α which gives the plant its natural ability to absorb the wind energy is examined. From the obtained plots, we remark that when α grows, the system bandwidth increases but the maximal amplitude at the resonance is unchanged. This result confirms what it is usually seen on the field where plants with large shape absorb easily the wind energy than those of small shape. Meanwhile the growth of the energy absorption parameter α increases the ability of the plant to enter the resonance state.

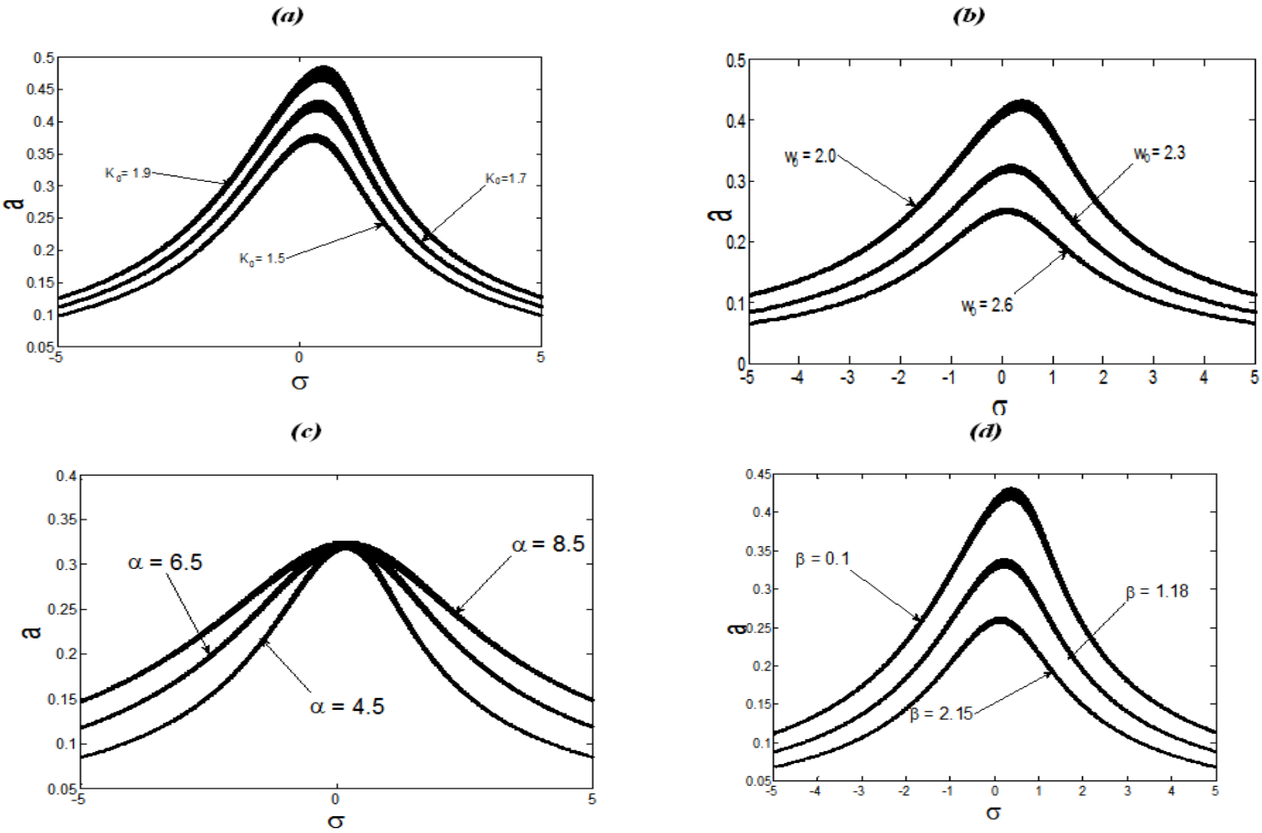

Figure 4. Effects of (a) the wind's load amplitude K_0, (b) the natural frequency of the plant ω_0, (c) the energy absorption parameter α, and (d) the plant density parameter β on the resonance curve for the parameters of Fig.2.

As Fig. 4(d) is concerned, we observe the effects of the parameter β (which links with the plant's density in the field) on the resonance behavior. It appears from the obtained curves that the resonance phenomenon is reducing as the values of β increase.

3.2.2. Stability State of the Primary Oscillations

In this subsection, we examine the stability of the nonlinear displacement of the plant suggested to the specific

wind loads. To build the stability criterion of the process, we assume that the stationary state suffers a small perturbation which manifests itself by slight variations of a and ψ as follows : $a = a_0 + a_1$ and $\psi = \psi_0 + \psi_1$ wherein a_0 and ψ_0 define the steady-state amplitude and phase while a_1 and ψ_1 are respectively their perturbations (with $a_1 << a_0$ and $\psi_1 << \psi_0$). Inserting a and ψ into the system (14) yields two differential equations that govern the evolution of the perturbation from which we derive the following eigen values equation :

$$\lambda^2 - (b_{11} + b_{22})\lambda + b_{11}b_{22} - b_{21}b_{12} = 0 \tag{16}$$

where λ designates an eigen value and the coefficients bij $(i, j = 1,2)$ are given in Appendix D. Application of the Routh-Hurwitz stability criterion yields the conditions for the stability of plant under the non-sinusoidal wind load :

$$-(b_{11} + b_{22}) > 0 \text{ and } b_{11}b_{22} - b_{21}b_{12} > 0 \tag{17}$$

The numerical resolution of Eq. (16) by verifying the simultaneous analytical condition (17) gives solution plotted on Figs. 5. These figures show that, for some values of the detuning parameter, the instability and the stability solutions are separated in certain area. Here, the system (plant-wind) exhibits a regular movement and the behavior of the plant can be easily controlled while this operation seems to be difficult in the regions were the instability and stability responses of the system are confused. Here, we are mostly concerned by mechanical stability because only stable solutions of dynamical systems are of interest since they correspond to the real position occupied by the system.

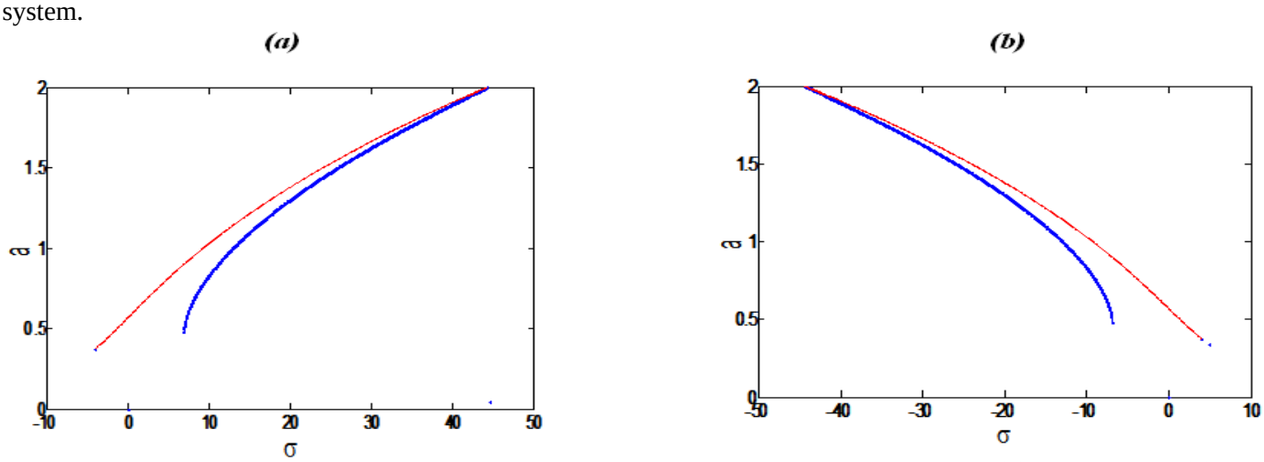

Figure-5. Stability curves of the harmonic oscillations of the system for the parameters of Fig. 2 with (a): $\gamma = 39$ and (b): $\gamma = -39$. The blue curve stands for the unstable solution and the red curves represent the stable solution.

3.2.3. Super-Harmonic Oscillations

When the wind amplitude K_0 is large, other types of behaviors could appear in the system known as sub-harmonics and super-harmonics resonant states. We will start our founding by the latter case. In order to express the closeness of ω to the internal frequency, we introduce the detuning parameter σ according to $\omega \approx (\omega_0/3) + \varepsilon^2\sigma$. Thus, additionally to the terms proportional to ($\exp\{i\omega_0 T_0\}$), the one proportional to ($\exp\{i(\omega_0 + 3\varepsilon^2\sigma)T_0\}$) also contribute. Therefore, the solvability condition is defined as:

$$\begin{aligned}&\left[i\omega_0\left(-\tfrac{2}{A_1}(dA_1/dT_1) - 2\mu_1 + 3A_1\overline{A_1}\left(i\gamma/\omega_0 - \alpha c_2\omega_0^2\right) - 3\alpha\alpha_2/2\right)\right]\exp\{i\omega_0 T_0\} \\ &+\tfrac{1}{8}c_2\alpha\left[\alpha_0(\beta_2\alpha_0 - 3i\alpha_2 - i\gamma_2\alpha_0) + \beta_0(\alpha_2 - \gamma_2\beta_0 + i\beta_2\beta_0)\right]\exp\{i(\omega_0 + 3\varepsilon^2\sigma)T_0\} = 0\end{aligned} \tag{18}$$

After substituting the expression of $A_1(T_1)$ taken in polar coordinates [21, 22] into Eq.(18), computations lead to the nonlinear equation below :

$$H_0 a^6 + H_1 a^4 + H_2 a^2 + H_3 = 0 \tag{19}$$

with $H_0 = b_1^2 + \frac{9}{64}\gamma^2$; $H_1 = 2\left[b_1(\mu_1\omega_0 + b_2) - \frac{9}{8}\omega_0\gamma\sigma\right]$;

$H_2 = \left[(\mu_1\omega_0 + b_2)^2 + 9\omega_0^2\sigma^2\right]$ and $H_3 = -(b_3^2 + b_4^2)$

in which $b_1 = 3\alpha\alpha_2\omega_0/4$; $b_2 = 3\alpha c_2\omega_0^3/8$; $b_3 = \frac{1}{8}c_2\alpha\left[\beta_2\alpha_0 + (\alpha_2 - \gamma_2)\beta_0\right]$ and

$b_4 = \frac{1}{8}c_2\alpha\left[\beta_2\beta_0 - (3\alpha_2 + \gamma_2)\alpha_0\right]$

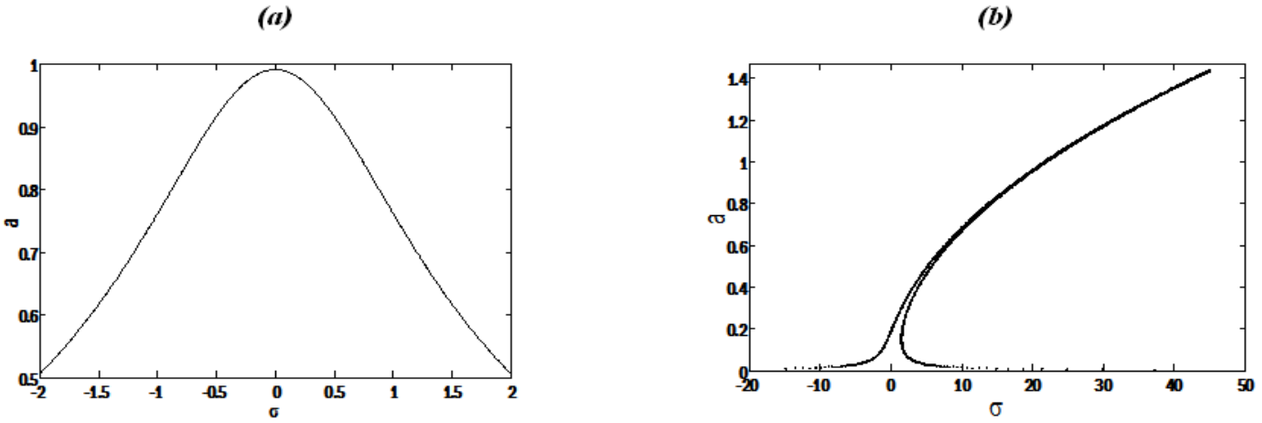

Figure-6. Resonance-curve and hysteresis of the super-harmonic behavior of the plant for the parameters $c_1 = 0.9$, $c_2 = 0.02$, $\beta = 8$, $\alpha = 3.6$, $k_0 = 6.37$, $\omega_0 = 0.5$, $\mu = 0.1$ with $\gamma = 5$ for resonance and $\gamma = 35$ for hysteresis.

The numerical solution of Eq. (19) gives the resonance curve plotted on Fig. 6a that shows the behavior of the plant under wind load. The corresponding hysteresis is given by Fig. 6b. Indeed, the plants can be considered as a plastic or stable mechanical structure growing in variable media [8, 23]. Moreover, plants should give proof of plasticity to face the adversity of environment and adjust their growth properties during their existence. This specific character is contrary to another living species particularly the animals which can run away while their environment becomes hostile.

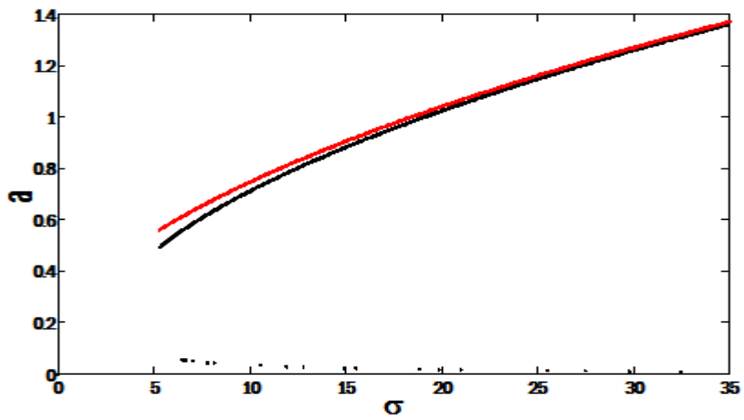

Figure-7. Stability curve for superharmonic oscillation obtain with the parameter of Fig. 6 with $\gamma = 55$. Stable solutions are in red color and unstable solutions in black color.

Following an analog method developed for the stability of primary oscillations, we show that the stability condition of super-harmonic oscillations deals with the sign of the eigen values of the equation :

$$\zeta^2 - (e_{11} + e_{22})\zeta + e_{11}e_{22} - e_{21}e_{12} = 0 \tag{20}$$

with the condition $-(e_{11} + e_{22}) > 0$ and $e_{11}e_{22} - e_{21}e_{12} > 0$ (21)

In Eq. (20), ζ designates an eigen value and the coefficients e_{ij} $(i, j = 1, 2)$ are given in Appendix E. The numerical solution of Eq. (20) is given on Fig. 7.

3.2.4. Sub-Harmonic Oscillation

To analyze the sub-harmonic resonance, we consider that the two frequencies are now linked by the relation $\omega = 3\omega_0 + \varepsilon^2\sigma$. Therefore the condition under which the secular terms are now cancelled is given by the relation :

$$\begin{aligned}\left\{i\omega_0\left[-2\left(dA_1/dT_1 + \mu_1 A_1\right) - 3\alpha A_1\left(\alpha_2/2 + c_2\omega_0^2 A_1\overline{A_1}\right)\right] - 3\gamma A_1^2\overline{A_1}\right\}\exp\{i\omega_0 T_0\} \\ + \left[\left(3\alpha c_2\omega_0^2\overline{A_1}^2\right)\Big/2\left(i\alpha_0 - \beta_0\right)\right]\exp\{i(\omega - 2\omega_0)T_0\} = 0\end{aligned} \tag{22}$$

After substitution of the expression of $A_1(T_1)$ defined by relation (11) into Eq.(22), we obtain the following system of equations

$$\begin{cases} h_2 a^2\cos\psi - h_3 a^2\sin\psi = -(\mu_1\omega_0 + h_1)a - ha^3 \\ -h_3 a^2\cos\psi - h_2 a^2\sin\psi = 3\gamma a^3/8 \end{cases} \tag{23}$$

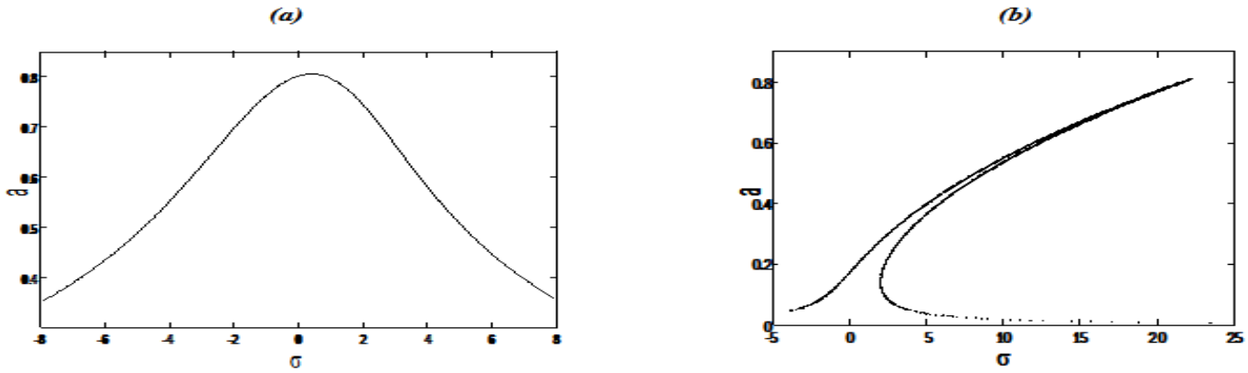

Figure-8. Frequency response curves and hysteresis of the sub-harmonic oscillations of the plant for the parameters : $c_1 = 0.6$, $c_2 = 0.1$, $\omega_0 = 0.18$, $K_0 = 2.78$, $\alpha = 5.02$, $\beta = 1.4$, $\mu = 0.4$ with $\gamma = 2.5$ for resonance (a) and $\gamma = 15$ for hysteresis (b).

that leads to the upcoming equation via some algebraic treatments :

$$A_0 a^4 + A_2 a^2 + A_3 = 0 \qquad (24)$$

with $A_0 = h^2 + 9\gamma^2/64$, $A_2 = 2h(\mu_1\omega_0 + h_1) - (h_2^2 + h_3^2)$ and $A_3 = (\mu_1\omega_0 + h_1)^2$ where $h = 3\alpha c_2 \omega_0^{\,3}/8$;

$h_1 = 3\alpha\alpha_2\omega_0/4$; $h_2 = 3\alpha c_2\omega_0^{\,2}\alpha_0/8$; $h_3 = 3\alpha c_2\omega_0^{\,2}\beta_0/8$ and $\psi = \sigma T_2 - 3\theta$

Numerical resolution of Eq. (24) yields solution that is plotted on Fig.8a with the corresponding hysteresis in Fig.8b. This numerical solution shows us the behavior of the amplitude ''a'' when the detuning parameter σ varies for some fixed values of the parameters K_0 and β.

From this figure, we can say that the resonance phenomenon occurs for the smallest values of some parameters than the super-harmonic oscillation. If we increase those parameters the plant can be destroyed.

According to the stability condition of sub-harmonic oscillation we have the following equation :

$$\kappa^2 - (q_{11} + q_{22})\kappa + q_{11}q_{22} - q_{21}q_{12} = 0 \qquad (25)$$

with the condition $-(q_{11} + q_{22}) > 0$ and $q_{11}q_{22} - q_{21}q_{12} > 0$ (26)

In this case, κ designates an eigen value and the coefficients q_{ij} $(i, j = 1, 2)$ are given in Appendix F. The solution of Eq. (25) is given on Fig.9 which shows that stable and unstable solutions are very confused as the detuning parameter σ exceeds a critical value. Thus, the plant motion cannot be controlled.

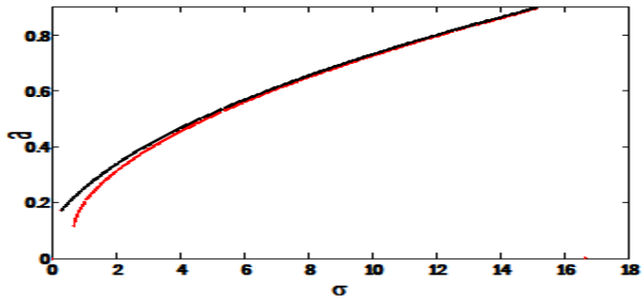

Figure-9. Stability curve for sub-harmonic oscillation obtain with the parameter of Fig. 8 with $\gamma = 25$. Stable solutions are in red color and unstable solutions in black color **;**

According to what appear in this part of our work and thanks to the fact that the variations of some parameters have a notorious effect on the system's dynamics, it becomes very interesting to see if the plant can be a seat of chaotic phenomenon.

4. Chaotic Behavior of the System

As nonlinear systems, trees under wind effects can exhibit chaotic motion depending on the perturbation of their initial state. Thus investigate how chaotic behavior arises in nonlinear systems is useful to complete the understanding of their behavior. Indeed, chaotic motions are of interest in executing activity adaptation [24] and state transitions in response to environmental changes [25] and, consequently create a rich repertory of responses [26]**.** The quenching of chaos in dynamical systems is also important in physical science because chaos control techniques are expected to bring out new phenomena in various scientific domains [27]**.** On the other hand, the existence of chaos is sometime needed because some chaotic dynamical systems have the advantage of providing qualitatively simple mechanism to generate deterministic pseudo randomness [28]**.** In applications, chaotic systems are used to produce, simulate and control different processes improving their performance or providing more suitable outputs [29]**.** Therefore the use of chaos in mechanical vibrating structures such as plants seems quite natural and assists to the introduction of constraints which aimed to elucidate the internal properties inherent to the system itself. In this section, we analyze the way chaos arises in the model described by Eqs.(2) since it is of interest in plant's oscillations.

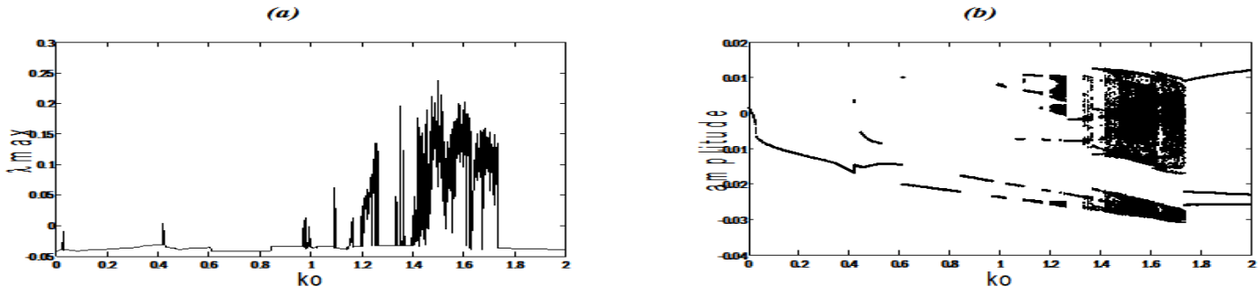

Figures-10. Lyapunov exponent (a) and bifurcation diagram (b) with the coefficients $\mu = 0.2$, $c_1 = 0.9$, $\beta = 0.01$, $\alpha = 5.0$, $\gamma = 0.1$, $\lambda = 0.2$ and $\omega_0 = 2.4$.

In the view of deriving the condition for the appearance of chaos in our model as the parameters of the system evolve, we start with the bifurcation analysis by rewriting (5) as combination of first order differential equations as follows:

$$\begin{cases} \dfrac{dx}{d\tau} = y \\ \dfrac{dy}{d\tau} = -\mu y - \alpha c_1 (y - z) - \left(\omega_0^2 x + \gamma x^3 + \lambda x^5\right) - \alpha c_2 \left(y^3 - z^3\right) - 3\alpha c_2 \left(y^2 z - z^2 y\right) \\ \dfrac{dz}{d\tau} = -\beta c_1 (y - z) - \beta c_2 \left(z^3 - y^3\right) + 3\beta c_2 \left(z^2 y - y^2 z\right) + k_0 \sin c(\omega t) \end{cases} \quad \textbf{(27)}$$

wherein x designates the amplitude of the plant motion, y stands for its speed and z represents the wind velocity.

Numerical resolution of Eq. (27) is made via the fourth-order Runge-Kutta algorithm using the wind amplitude K_0 as control parameter. Then the resulting bifurcation diagram and the variation of the corresponding Lyapunov exponent are given as K_0 varies (Figs. 10). Our investigation shows that the system exhibits chaotic behaviors only for large values of K_0. The phase portraits are depicted on Figs.11 showing both regular and chaotic motions for different values of K_0. We also observe form those graphs that the plant motion under non-sinusoidal wind effects present intermittence behavior.

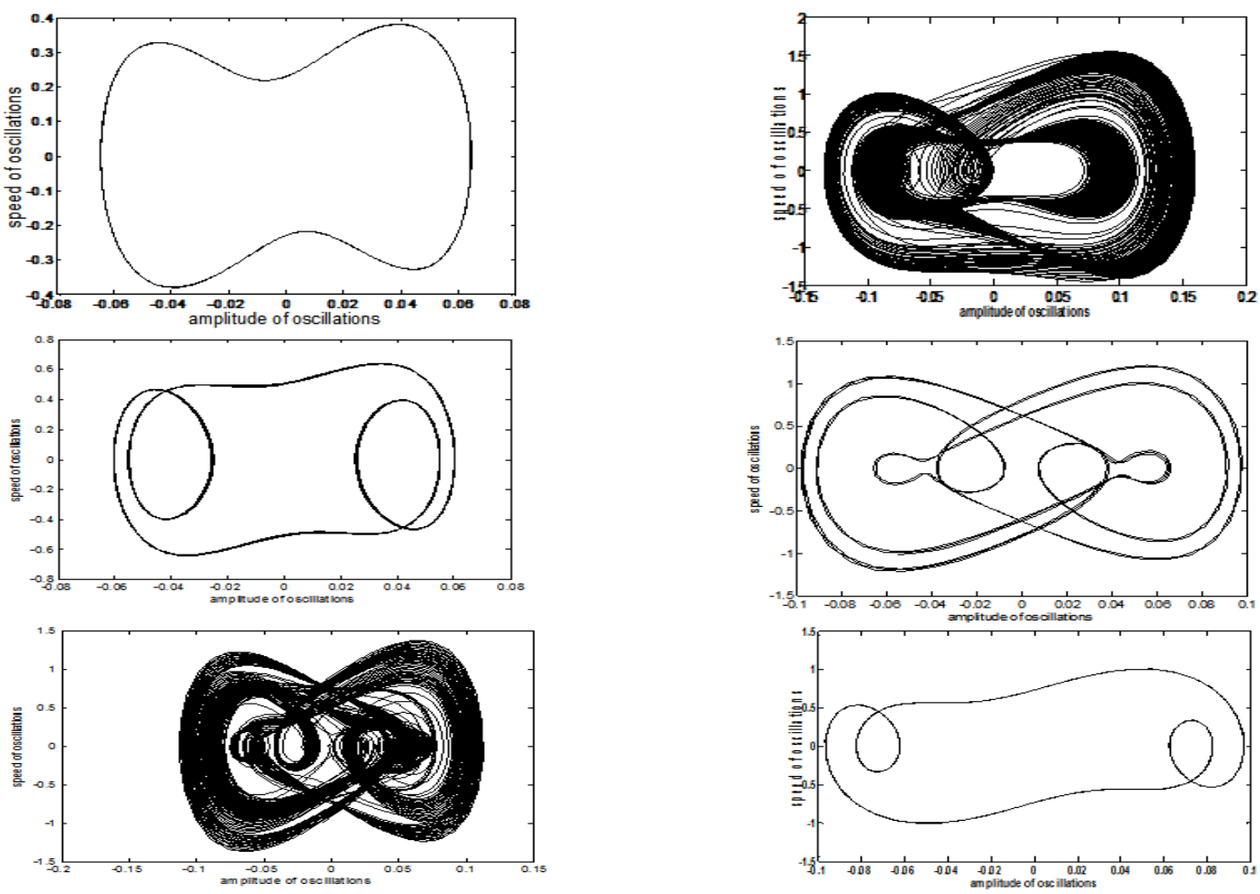

Figures 11. Phase portrait curves versus control parameters for (a) $K_0 = 0.282$; (b) $K_0 = 1.250$; (c) $K_0 = 1.310$; (d) $K_0 = 1.450$; (e) $K_0 = 1.799$ and (f) $K_0 = 1.990$.

Hereafter, we choose some specific plants or trees for possible applications of the results previously established. For those species, we examine the amplitude response, the corresponding hysteresis and the stability curves for the harmonic motion. The curves are obtained using the physical characteristics [4, 30, 31] of the maritime pine tree

(Figs.12), the corn plant (Figs.13) and the bamboo of raphia vinifera (Figs.14). All those plots show the behavior of those plants under wind loads. The chaotic behaviors of those species are not found.

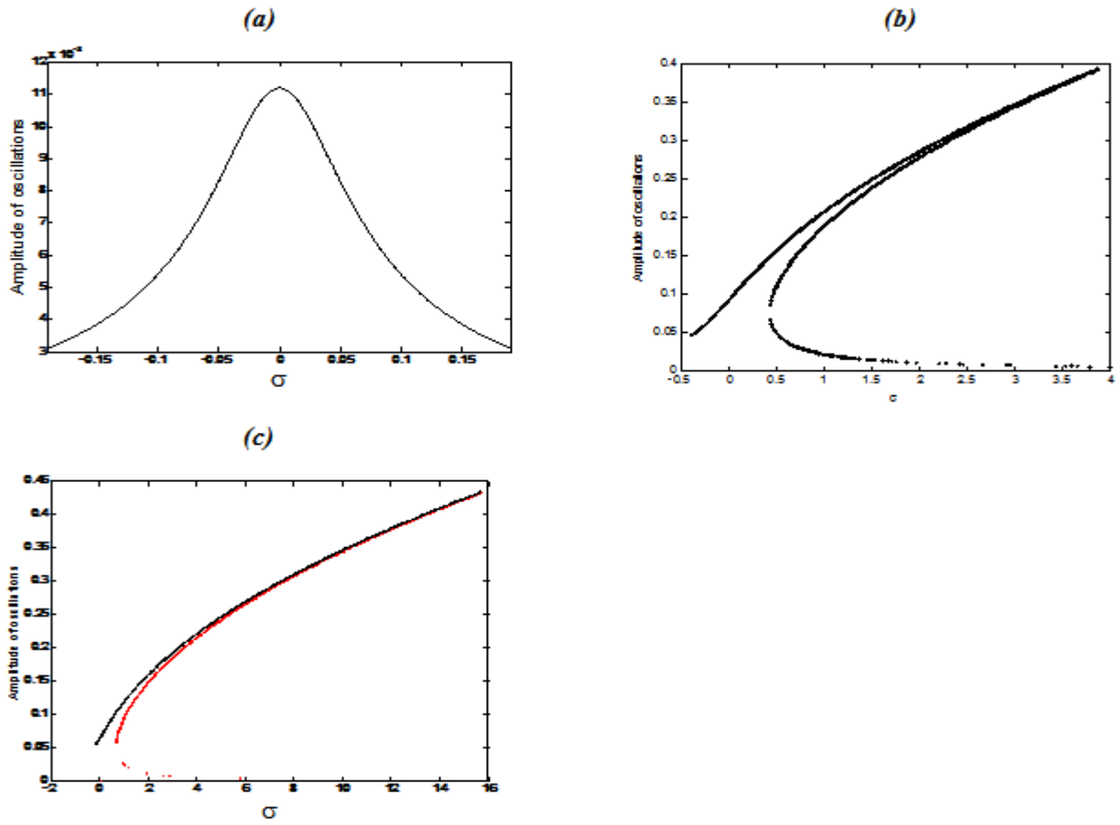

Figures 12. Resonance-curve (a), hysteresis (b) and stability (c) of the pine for the parameters $c_1 = 0.9$; $c_2 = 0.1$; $\mu = 0.05$; $\alpha = 0.1$; $\beta = 3.1$; $K_0 = 1.7$; $\omega_0 = 10.98$ with $\gamma = 120$ for resonance and $\alpha = 0.009$; $\beta = 0.02$; $\gamma = 200$ for hysteresis and stability (stable solution in black color and unstable solution in red color in Fig. 12c).

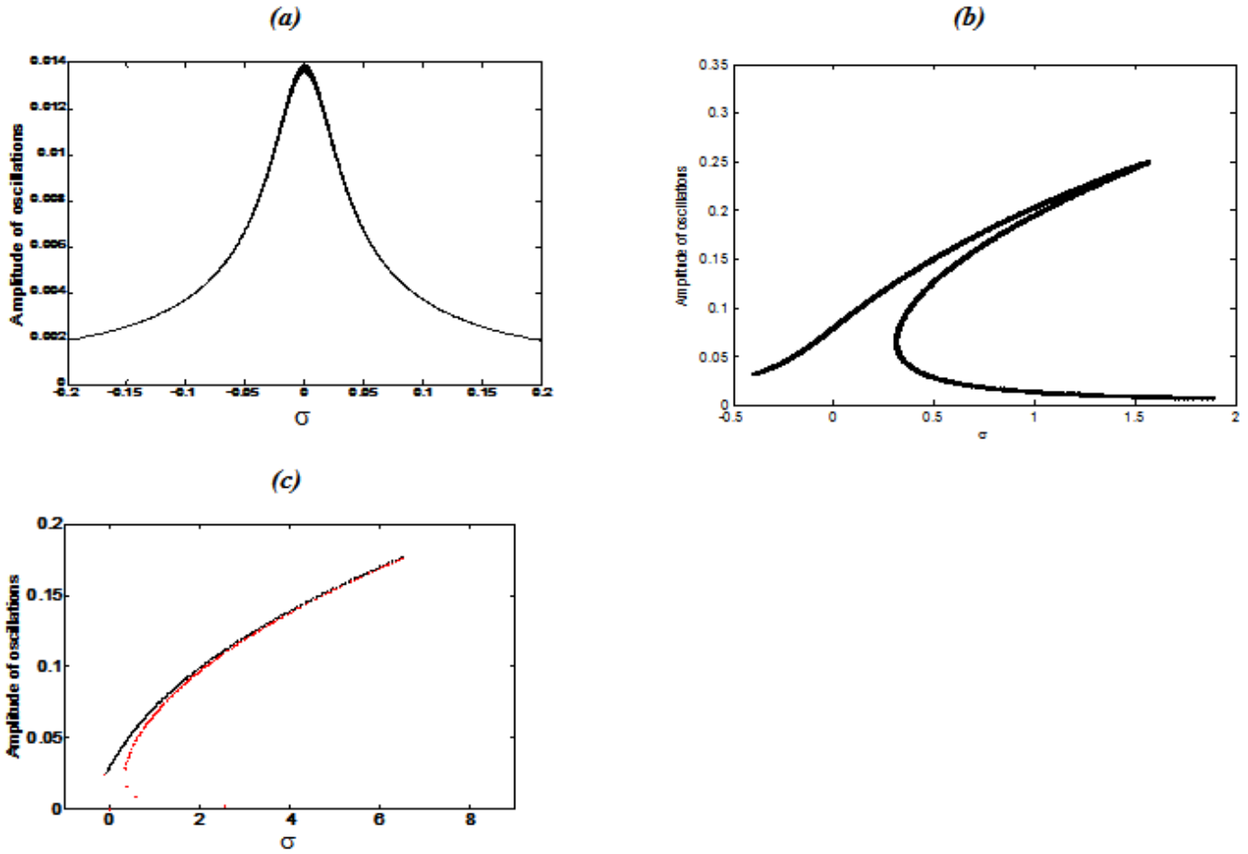

Figures-13. Resonance-curve (a), hysteresis (b) and stability (c) of corn for the parameters $c_1 = 0.9$; $c_2 = 0.1$; $\mu = 0.05$; $\alpha = 0.005$; $\beta = 0.5$; $K_0 = 1.7$; $\omega_0 = 10.98$ with $\gamma = 20$ for resonance and $\alpha = 0.002$; $\beta = 0.02$; $\gamma = 50$ for hysteresis and stability (stable solution in black color and unstable solution in red color in Fig. 13c).

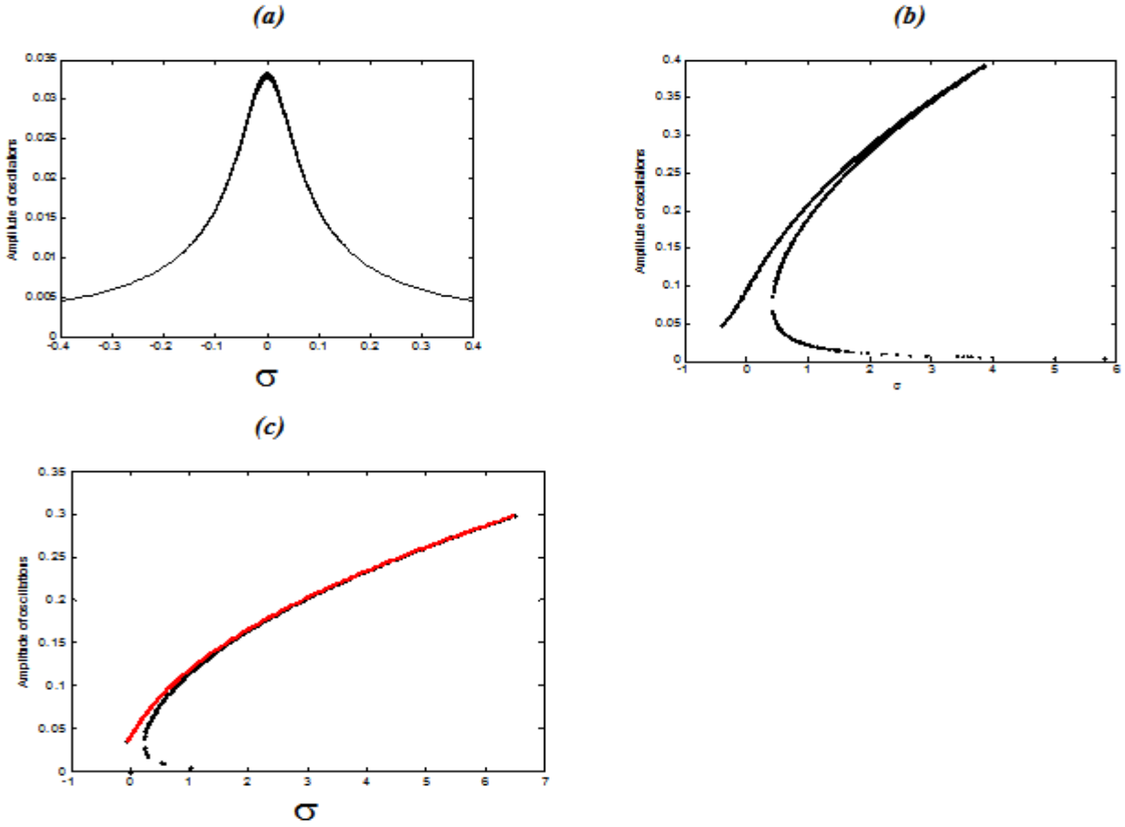

Figures 14. Resonance-curve (a), hysteresis (b) and stability (c) of bamboo with parameters $c_1 = 0.9$; $c_2 = 0.1$; $\mu = 0.02$; $\alpha = 0.1$; $\beta = 0.5$; $K_0 = 0.5$; $\omega_0 = 10.98$ with $\gamma = 2$ for resonance and $\alpha = \beta = 0.002$; $K_0 = 1.7$; $\omega_0 = 0.9$; $\gamma = 17$ for hysteresis and stability (stable solutions are in black color and unstable solutions in red color on Fig. 14c).

5. Conclusion

In this paper, we have studied the dynamics of plant suggested to non-sinusoidal wind loads. We have presented the features of considering a non-sinusoidal wind load instead of a sinusoidal wind profile. Different interesting nonlinear dynamics of the system (plant-wind) have been discussed analytically and numerically. For the resonant stationary state, we have observed several behaviors such as perfect resonant, hysteresis and quenching phenomenon of the plants motion under forced oscillations. The stability of harmonic, superharmonic and subharmonic oscillations has been analyzed and the obtained curves have exhibited the regions of stable and unstable behaviors. Within these results, we have noted the crucial role played by the cubic nonlinear coefficient on the system's dynamics has been perceived. We have also investigated the chaotic behavior of the plant subjected to a non-sinusoidal wind effects. Furthermore, we have shown the existence of regular and chaotic states that appear in discontinuous intervals leading to the intermittence phenomenon. For practical purposes, we have extended this study to various plant species such as maritime pine tree, corn plant and bamboo of raphia vinifera and, obtained goods results. Owing to the knowledge of the different structures and to the cropping method developed, all these results could be exploited in agriculture for the harmonious development of plants in the field (or trees in the forest).

Appendix-A. Coefficients of equation (9)

$$M_1 = -2i\omega_0\left(\frac{dA_1}{dT_1} + \mu_1 A_1 + \frac{3}{4}\alpha\alpha_2 A_1\right) - 3A_1^2\overline{A}_1\left(\gamma + \alpha c_2 {\omega_0}^3\right)$$

$$M_2 = -\frac{\alpha_0\alpha c_2}{8}\left(i\alpha_2 + \beta_2 + i\gamma_2 + 24i{\omega_0}^2 A_1\overline{A}_1\right); \quad M_3 = -\frac{\beta_0\alpha c_2}{8}\left(\alpha_2 - i\beta_2 + 3\gamma_2 + 24{\omega_0}^2 A_1\overline{A}_1\right)$$

$$M_4 = \frac{c_2\alpha\alpha_0}{8}\left(-3i\alpha_2 + \beta_2 - i\gamma_2\right); \quad M_5 = \frac{c_2\alpha\beta_0}{8}\left(\alpha_2 + i\beta_2 - \gamma_2\right)$$

$$M_6 = A_1^3(-\gamma + ic_2\alpha\omega_0^3); \quad M_7 = \frac{3}{4}\alpha c_2\omega_0 A_1\left(\alpha_2 i + \beta_2 + \gamma_2 i\right); \quad M_8 = \frac{3}{2}\alpha c_2{\omega_0}^2 A_1\left(iA_1\alpha_0 + \beta_0\right)$$

$$M_9 = 3\alpha c_2{\omega_0}^2\overline{A}_1^2\left(\frac{1}{2}\beta_0 - \alpha_0\right); \quad M_{10} = \frac{3}{4}\alpha c_2\omega_0\overline{A}_1 i\left(\beta_2 - \alpha_2 - \gamma_2\right).$$

with

$$\alpha_2 = \frac{1}{\omega^2}\left(\alpha_{11} + \frac{\alpha_{12}}{\omega} + \frac{\alpha_{13}}{\omega^2}\right); \quad \beta_2 = \frac{\beta_{11}}{\omega^4} + \frac{\beta_{12}}{\omega^3} + \frac{\beta_{13}}{\omega^2} + \frac{\beta_{14}}{\omega} \quad \text{and} \quad \gamma_2 = \frac{\gamma_{11}}{\omega^4} + \frac{\gamma_{12}}{\omega^2} + \gamma_{13}$$

in which

$$\alpha_{11}=\frac{K_0^{\,2}}{T_0^{\,2}c_1^{\,4}}\left(\frac{1}{\beta^2}+\frac{2}{T_0c_1\beta}+\frac{1}{T_0^{\,2}c_1^{\,2}}\right)\quad;\quad \alpha_{12}=\frac{2K_0^{\,2}}{c_1^{\,2}T_0^{\,2}}\left(1+\frac{(\beta^2-1)}{T_0c_1\beta}-\frac{1}{T_0^{\,2}c_1^{\,2}}\right)\quad;\quad \alpha_{13}=\frac{K_0^{\,2}}{T_0}\left(\beta^2-\frac{2\beta}{T_0^{\,2}c_1}+\frac{1}{T_0^{\,3}c_1^{\,2}}\right)\quad;$$

$$\beta_{11}=-\frac{2K_0^2}{T_0^2c_1}\left(\beta-\frac{1}{T_0c_1}\right);\quad \beta_{13}=-\frac{2K_0^2}{T_0^2c_1^2}\left(1+\frac{2\beta}{T_0c_1}+\frac{2\beta}{T_0c_1^2}-\frac{1}{T_0c_1\beta^2}-\frac{2\beta}{T_0^2c_1^2}-\frac{2}{T_0^2c_1^3}\right);$$

$$\beta_{12}=-\frac{2K_0^2}{T_0^2c_1}\left(\frac{1}{\beta c_1}+\frac{1}{T_0}\right);\quad \beta_{14}=-\frac{2K_0^2}{T_0^2c_1^4}\left(\frac{1}{\beta}+\frac{2}{T_0c_1}+\frac{2}{T_0\beta c_1^2}+\frac{1}{T_0c_1\beta}+\frac{2\beta}{T_0^2c_1^2}+\frac{2}{T_0^2c_1^3}\right)$$

$$\gamma_{11}=\frac{K_0^{\,2}}{T_0^{\,2}c_1^{\,2}};\quad \gamma_{12}=\frac{2K_0^{\,2}}{T_0^{\,2}c_1^{\,3}}\left(\frac{1}{\beta^2}+\frac{2\beta}{T_0c_1}+\frac{2}{c_1^{\,2}}\right);\gamma_{13}=\frac{4K_0^{\,2}}{T_0^{\,2}c_1^{\,4}}\left(\frac{4}{\beta^4}+\frac{1}{T_0\beta c_1}+\frac{1}{T_0\beta^2c_1^{\,2}}+\frac{\beta^2}{T_0^{\,2}c_1^{\,2}}+\frac{2\beta}{T_0^{\,2}c_1^{\,3}}+\frac{T_0^{\,2}}{c_1^{\,4}}\right);$$

Appendix-B. Coefficients of equation (14)

$$d_0=\frac{3}{4}\alpha\alpha_2;\ d_1=\frac{1}{8\omega_0}\alpha\alpha_2c_2\alpha_0;\ d_2=\frac{1}{8\omega_0}\alpha\alpha_2c_2\beta_0;\ d_3=\frac{1}{8\omega_0}\alpha\beta_2c_2\alpha_0;\ d_4=\frac{1}{8\omega_0}\alpha\beta_2c_2\beta_0;\ d_5=\frac{1}{8\omega_0}\alpha\gamma_2c_2\alpha_0;$$

$$d_6=\frac{3}{8\omega_0}\alpha\gamma_2c_2\beta_0;\ d_7=\frac{3}{4}\alpha c_2\omega_0\beta_0;\ d_8=\frac{3}{4}\alpha c_2\omega_0\alpha_0;\ d_9=\frac{3}{8}\alpha c_2\left(\alpha_2+\beta_2+\gamma_2\right);\ \text{With}\quad f_1=d_4-d_5\quad;$$

$$f_2=d_2+d_6\ ;\qquad g_1=f_1-d_1\ ;\qquad g_2=f_2+d_3\ ;\quad \eta_2=\sigma a-\frac{3}{8\omega_0}\gamma a^3\ ;\qquad \psi=\sigma T_2-\theta\ ;$$

$$\eta_1=\left(\mu_1+d_0\right)a+\frac{3}{8}\omega_0^2\alpha c_2a^3$$

Appendix-C. Coefficients of equation (15)

$$A_0=\frac{9}{64}\left(\omega_0^4\alpha^2c_2^2-\frac{\gamma^2}{\omega_0^2}\right);\quad A_2=\frac{3}{4}\left[\omega_0^2\alpha c_2\left(\mu_1+d_0\right)+\frac{\gamma}{\omega_0^2}\sigma\right]+d_7^2+d_8^2\ ;$$

$$A_{11}=-\frac{3}{4}\left(d_8\omega_0^2\alpha c_2-\frac{d_7\gamma}{\omega_0}\right)\cos\left(\psi\right)+\frac{3}{4}\left(\frac{d_8\gamma}{\omega_0}-d_7\omega_0^2\alpha c_2\right)\sin\left(\psi\right)\ ;$$

$$A_3=\left[\frac{3}{4}\left(g_1\omega_0^2\alpha c_2-\frac{\gamma}{2\omega_0}g_2\right)+2\left(d_7\sigma-d_8\left(\mu_1+d_0\right)\right)\right]\cos\left(\psi\right)$$
$$-\left[\frac{3}{4}\left(g_2\omega_0^2\alpha c_2+\frac{\gamma}{\omega_0}g_1\right)+2\left(d_8\sigma+d_7\left(\mu_1+d_0\right)\right)\right]\sin\left(\psi\right)\ ;$$

$$A_4=\left(\mu_1+d_0\right)^2-d_9^2+\sigma^2+2\left(d_7g_2-d_8g_1\right)\quad;$$

$$A_5=\left[2\left(g_2\sigma+g_1\left(\mu_1+d_0\right)\right)\right]\cos\left(\psi\right)+\left[2\left(g_1\sigma-g_2\left(\mu_1+d_0\right)\right)\right]\sin\left(\psi\right)\ ;$$

$$A_6=g_1^2+g_2^2$$

Appendix-D. Coefficients of equation (16)

$$b_{11}=\left(\mu_1+d_0\right)+\frac{9}{8}\omega_0^2\alpha c_2a_0^2-2d_8a_0^2\cos\left(\psi_0\right)-2d_7a_0\sin\left(\psi_0\right)-d_9\cos\left(2\psi_0\right);$$

$$b_{12}=-\left(g_1-d_8a_0^2\right)\sin\left(\psi_0\right)-\left(g_2+d_7a_0^2\right)\cos\left(\psi_0\right)+2d_9a_0\sin\left(2\psi_0\right);$$

$$b_{21}=\sigma-\frac{9\gamma a_0^2}{8\omega_0}+2d_8a_0^2\sin\left(\psi_0\right)-2d_7a_0\cos\left(\psi_0\right)+d_9\sin\left(2\psi_0\right);$$

$$b_{22}=-\left(g_1-d_8a_0^2\right)\cos\left(\psi_0\right)+\left(g_2+d_7a_0^2\right)\sin\left(\psi_0\right)+2d_9a_0\cos\left(2\psi_0\right)$$

Appendix-E. Coefficients of equation (20)

$$e_{11}=\mu_1+\frac{b_2}{\omega_0}+\frac{3b_1}{\omega_0}a_0^2\quad;\quad e_{12}=\frac{1}{\omega_0}\left(b_3\cos\psi_0-b_4\sin\psi_0\right)\quad;\quad e_{21}=\frac{3}{4\omega_0}\gamma a_0-\frac{1}{\omega_0a_0^2}\left(b_3\cos\psi_0-b_4\sin\psi_0\right)\quad\text{and}$$

$$e_{22}=-\frac{1}{\omega_0a_0}\left(b_3\sin\psi_0+b_4\cos\psi_0\right)\quad\text{with}\quad b_1=\frac{3}{4}\alpha\alpha'\omega_0\ ,\ b_2=\frac{3}{8}\alpha c_2{\omega_0}^3\ ,$$

$$b_3=\frac{1}{8T_0}c_2\alpha\left[\left(\alpha'-\gamma'\right)\left(\left(B+K\right)+\frac{\eta-\xi}{T_0}\right)+\beta'\left(\left(A+D\right)+\frac{F-B}{T_0}\right)\right]\quad,$$

$$b_4=\frac{1}{8T_0}c_2\alpha\left[\beta'\left(\left(B+K\right)+\frac{\eta-\xi}{T_0}\right)-\left(3\alpha'+\gamma'\right)\left(\left(A+D\right)+\frac{F-B}{T_0}\right)\right]$$

Appendix-F. Coefficients of equation (25)

$$q_{12} = \frac{1}{\omega_0}\left(h_3 \cos\psi_0 - h_2 \sin\psi_0\right);\ q_{21} = \frac{3}{8\omega_0}\gamma a_0 + a_0^2\left(h_3 \cos\psi_0 + h_2 \sin\psi_0\right)$$

and $$q_{22} = a_0^2\left(h_2 \cos\psi_0 + h_3 \sin\psi_0\right).$$

with $$h = \frac{3}{8}\alpha c_2 \omega_0^{\ 3};\ h_1 = \frac{3}{4}\alpha\alpha'\omega_0\ ;\qquad h_2 = \frac{3}{8}\alpha c_2 \omega_0^{\ 2}\left(\frac{A+D}{T_0} + \frac{F-B}{T_0^2}\right)$$

and $$h_3 = \frac{3}{8}\alpha c_2 \omega_0^{\ 2}\left(\frac{B+K}{T_0} + \frac{\eta+\xi}{T_0^2}\right).$$

References

[1] E. M. Everham, *A comparison of methods for quantifying catastrophic wind damage to forests. In Wind and Trees, M.P. Coutts and J. Grace, Ed*. Cambridge: Cambridge University Press, 1995.

[2] J. J. Finnigan, "Turbulence in plant canopies," *Annu. Rev. Fluid Mech.,* vol. 32, pp. 519-571. Available http://dx.doi.org/10.1146/annurev.fluid.32.1.519, 2000.

[3] M. Denny, B. Gaylord, B. Helmuth, and T. Daniel, "The menace of momentum: Dynamic forces on flexible organisms," *Limnol. Oceanogr*, vol. 43, pp. 955-968. Available http://dx.doi.org/10.4319/lo.1998.43.5.0955, 1998.

[4] S. Damien and F. Thierry, "A mechanical analysis of the relationship between free oscillations of pinus pinaster ait. Saplings and their aerial architecture," *J. Exp. Bota.,* vol. 56, pp. 1563-1573. Available http://dx.doi.org/10.1093/jxb/eri151, 2005.

[5] H. Wandeler and R. Günter, "Lagebeurteilung aus der sicht der eidgenössischen forstdirektion," *Schweiz Z Forstwes,* vol. 142, pp. 453-462, 1991.

[6] J. L. Haymond, D. D. Hook, and W. R. Harms, "South Carolina forest land research and management related to the storm," USDA Forest Service Southern Research Station Gen. Tech. Rep. SRS-5, 1996.

[7] C. Mattheck and H. Breloer, *The body language of trees*. London: HMSO, 1994.

[8] C. Py, "Couplage entre la dynamique du vent et le mouvement d'un couvert végétal," PhD Thesis, Université Paris VI Pierre et Marie Curie, 2005.

[9] R. Baile, "Analyse et modélisation multi-fractales de vitesses de vent. Application a la prévision de la source éolienne," PhD Thesis, Université de Corse, 2010.

[10] C. J. Wood, *Understanding wind forces on trees. In: Wind and trees, M.P. Coutts and J. Grace, Ed*. Cambridge: Cambridge University Press, 1995.

[11] K. James, "Dynamic loading of trees," *Journal of Arboriculture,* vol. 29, pp. 165-171, 2003.

[12] R. Tchassi, "Application de la théorie des oscillations a l'étude de l'écoulement du vent sur les voutes végétales oscillatoires," Master Thesis, Université de Dschang, Cameroun, 1998.

[13] P. K. Talla, J. S. Mabekou, A. Fomethe, G. L. Gbaguidi Aisse, G. N. Bawe, E. Foadieng, and A. Fougjet, "Nonlinear dynamic of plants vibrating under wind effects," *Inter. J. Theo. Applied Mech.,* vol. 6, pp. 19-36. Available www.ripublication.com/Volume/ijtamv6n1.htm, 2011.

[14] E. T. Whittaker, "On the functions which are represented by the expansion of interpolating theory," *Proc. Royal Soc. of Edinburgh,* vol. 35, pp. 181-194. Available http://dx.doi.org/10.1017/S0370164600017806, 1915.

[15] J. M. Whittaker, *Interpolatory function theory*. Cambridge University Press, Coll. Cambridge Tracts in Mathematics and Mathematical Physics, 1935.

[16] F. Stenger, "Numerical methods based on sinc and analytic functions," *Mathematics of Computation,* vol. 63, pp. 817-819. Available http://dx.doi.org/10.2307/2153301, 1994.

[17] R. Bracewell, *The filtering or interpolating function, in the fourier transform and its applications*, 3rd ed. New York: McGraw-Hill, 1999.

[18] A. H. Nayfeh and D. T. Mook, *Nonlinear oscillations*. New York: Willey Intersciences, 1996.

[19] K. E. Morrison, "Cosine products, fourier transforms, and random sum," *Amer. Math. Monthly,* vol. 102, pp. 716-724. Available http://dx.doi.org/10.2307/2974641, 1995.

[20] C. Jutten, *Théorie du signal, cours de 2eme année*: Université Joseph Fourier- Polytech'Grenoble. Available www.gipsa-lab.grenoble-inp.fr/...jutten/mescours/Theorie_du_signal.pdf, 2009.

[21] E. De Langre, "Effects of wind on plants," *Annual Review of Fluid Mechanics,* vol. 40, pp. 141-168. Available http://dx.doi.org/10.1146/annurev.fluid.40.111406.102135, 2008.

[22] R. Mathieu, "Evolution et organisation spatiale de la dynamique vibratoire des arbres au cours de leur développement," PhD Thesis, Université Paris VI Pierre et Marie Curie, 2009.

[23] C. Py, E. De Langre, and B. Moulia, "A frequency lock-in mechanism in the interaction between wind and crop canopies," *J. Fluid Mech.,* vol. 568, pp. 425- 449. Available http://dx.doi.org/10.1017/S0022112006002667, 2006.

[24] M. Rodriguez, E. De Langre, and B. Moulia, "A scaling law for the effects of architecture and allometry on tree vibration modes suggests a biological tuning to modal compartmentalization," *American Journal of Botany,* vol. 95, pp. 1523-1537. Available http://dx.doi.org/10.3732/ajb.0800161, 2008.

[25] F. Bruchert, O. Speck, and H. C. Spatz, "Oscillations of plants' stems and their damping: Theory and experimentation," *Philos. Trans. R. Soc. B.,* vol. 358, p. 1487. Available http://dx.doi.org/10.1098/rstb.2003.1348, 2003.

[26] A. Kimiaeifar, E. Lund, O. T. Thomsen, and A. Barari, "On the approximate analytical solution of nonlinear vibrations of inextensible beams using high parameter-expansion method," *International Journal of Nonlinear Sciences and Numerical Simulation,* vol. 11, pp. 743-753, 2011.

[27] O. C. Pinto and P. B. Goncalves, "Active non-linear control of buckling and vibrations of a flexible buckled beam," *Chaos Solitons and Fractals,* vol. 14, pp. 227-239. Doi: 10.1016/S0960-0779(01)00229-6, 2002.

[28] W. Zhang, "Chaotic motion and its control for nonlinear nonplanar oscillations of a parametrically excited cantilever beam," *Chaos Solitons and Fractals,* vol. 26, pp. 731-745. Available http://dx.doi.org/10.1016/j.chaos.2005.01.042, 2005.

[29] S. L. T. De Souza and I. L. Caldas, "Controlling chaotic orbits in mechanical systems with impacts," *Chaos Solitons and Fractals,* vol. 19, pp. 171-178. Available http://dx.doi.org/10.1016/S0960-0779(03)00129-2, 2004.

[30] V. Cucchi, C. Meredieu, A. Stokes, F. Coligny, J. Suarez, and B. Gardiner, "Modelling the windthrow risk for simulated forest stands of maritime pine (Pinus Pinaster Ait.)," *Forest Ecol. Manag.,* vol. 213, pp. 184-196. Available http://dx.doi.org/10.1016/j.foreco.2005.03.019, 2005.

[31] P. K. Talla, E. Foadieng, M. Fogue, J. S. Mabekou, F. B. Pelap, A. F. Sinju, and A. Foudjet, "Nonlinear creep behavior of raphia vinifera L. Arecacea under flexural load," *Journal of Mechanics and Solids,* vol. 5, pp. 151-172. Available www.ripublication.com/Volume/ijmsv5n2.htm, 2010.

Views and opinions expressed in this article are the views and opinions of the authors, Asian Engineering Review shall not be responsible or answerable for any loss, damage or liability etc. caused in relation to/arising out of the use of the content.